

Verification of functional a posteriori error estimates for a contact problem in 1D

P. HARASIM, J. VALDMAN*

Centre of Excellence IT4Innovations,
VŠB-Technical University of Ostrava,
Czech Republic

January 28, 2013

Abstract

We verify functional a posteriori error estimates of numerical solutions of a contact problem in 1D. The contact problem is described by a quadratic minimization problem with a bound constrain and it can be equivalently formulated as a variational inequality. The simplification into 1D allows for the construction of a benchmark for which an exact solution can be derived. Numerical solution obtained by the finite element method can be compared with the exact solution and their difference is further estimated in the energetic norm by a functional majorant proposed by Repin et al. Numerical tests provide sharp estimation of the approximation error.

1 Formulation of contact problem in 1D

We will deal with a state problem motivated by the following linear boundary value problem: Find a function u such that

$$-u'' = f \quad \text{in } (0, 1) \quad (1)$$

$$u(0) = u(1) = 0, \quad (2)$$

where f is a continuous right-hand side, $f < 0$. Equation (1) describe, for instance, the elastic deformation of a string. Here, f stands for an external force density. If an obstacle ϕ is added, see Figure 1, then a contact problem for elastic deformation of string arises. This problem is typically described by a variational inequality equivalent to the following minimization problem:

Problem 1 (minimization problem). Find $u \in K$ satisfying

$$J(u) = \inf_{v \in K} J(v), \quad (3)$$

where the energy functional reads

$$J(v) := \frac{1}{2} \int_0^1 (v')^2 dx - \int_0^1 f v dx \quad (4)$$

and the admissible set is defined as

$$K := \{v \in V_0 : v(x) \geq \phi(x) \text{ a.e. in } (0, 1)\},$$

where $f \in L^2(0, 1)$, V_0 denote the standard Sobolev space $H_0^1(0, 1)$ and $\phi \in H^1(0, 1)$ such that $\phi \notin V_0$ and $\phi(x) < 0$ a.e. in $(0, 1)$.

*corresponding author, email: jan.valdman@vsb.cz

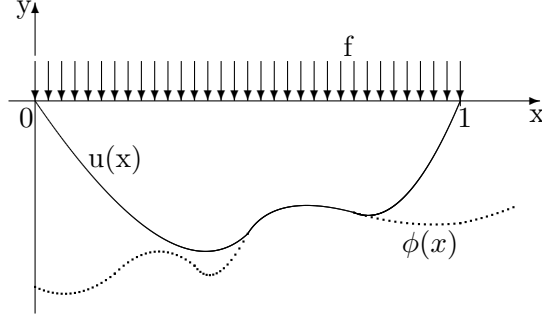


Figure 1: Illustration of the contact problem.

Problem 1 is a quadratic minimization problem with a convex constrain and the existence of its minimizer is guaranteed by the Lions- Stampacchia Theorem [4]. It is also equivalent to the variational inequality: Find $u \in K$ such that

$$\int_0^1 u'(v-u)'dx \geq \int_0^1 f(v-u)dx \quad \text{for all } v \in K. \quad (5)$$

The convex constrain $v \in K$ can be transformed into a linear term containing a new (Lagrange) variable in *Problem 2* (Perturbed problem). Let $W := \{v + t\phi : v \in V_0 \text{ and } t \in \mathbb{R}\} \subset H^1(0,1)$, where \mathbb{R} stands for set of real number. For given

$$\mu \in \Lambda := \{\mu \in W^* : \langle \mu, v - \phi \rangle \geq 0 \text{ for all } v \in K\} \quad (6)$$

find $u_\mu \in V_0$ such that

$$J_\mu(u_\mu) = \inf_{v \in V_0} J_\mu(v), \quad (7)$$

where W^* denote the dual space of W and the perturbed functional J_μ is defined as

$$J_\mu(v) := J(v) - \langle \mu, v - \phi \rangle. \quad (8)$$

Problems 1 and 2 are related and it obviously holds

$$J_\mu(u_\mu) \leq J(u) \quad \text{for all } \mu \in \Lambda. \quad (9)$$

Lemma 1 (Existence of optimal multiplier). There exists $\lambda \in \Lambda$ such that

$$u_\lambda = u \quad (10)$$

and

$$J_\lambda(u) = J(u). \quad (11)$$

Proof. Obviously, W is the least linear subspace of $H^1(0,1)$ such that definition (8) of perturbed functional J_μ is correct. Let $w \in W$ is arbitrary. We decompose

$$w = v + t\phi, \quad (12)$$

where $v \in V_0$ and $t \in \mathbb{R}$ and this decomposition can be shown to be unique. Now, we define a functional λ as follows:

$$\langle \lambda, w \rangle := \int_0^1 u'v'dx - \int_0^1 fvdxdx + t \left[\int_0^1 (u')^2 dx - \int_0^1 fudxdx \right]. \quad (13)$$

We assert that the functional defined by (13) has required properties (10) and (11). Apparently, λ is a linear functional on W . The functional λ is also continuous. It is a consequence of continuity of decomposition (12), which can be proved as follows. Let $w \in W$ is arbitrary and $w_n \rightarrow w$ in W , where $w_n \in W$. With

respect of (12), we can write $w_n = v_n + t_n \phi$ and $w = v + t \phi$, where $v_n, v \in V_0$ and $t_n, t \in \mathbb{R}$. As a consequence of unique orthogonal decomposition of ϕ we infer

$$\|w_n - w\|_{H^1(0,1)} \geq |t_n - t| \|\phi^\perp\|_{H^1(0,1)},$$

where ϕ^\perp is the component of ϕ orthogonal to subspace V_0 . Moreover, it follows from the triangle inequality that

$$\|v_n - v\|_{H^1(0,1)} \leq \|w_n - w\|_{H^1(0,1)} + |t_n - t| \|\phi\|_{H^1(0,1)}.$$

Consequently, $v_n \rightarrow v$ in W and $t_n \rightarrow t$. Now, if we restrict the space W to the origin V_0 , we obtain

$$\langle \lambda, w \rangle := \int_0^1 u' v' dx - \int_0^1 f v dx \quad \text{for all } w \in V_0, \quad (14)$$

which is equivalent to the property (10), i.e., $\inf_{w \in V_0} J_\lambda(w) = J_\lambda(u)$. Furthermore, if we take $w = u - \phi$, it follows from (13) that

$$\langle \lambda, u - \phi \rangle = \langle \lambda, u \rangle - \langle \lambda, \phi \rangle = 0$$

and consequently the property (11) is fulfilled. Finally, we verify the condition of nonnegativity from definition (6). Let $v \in K$ is arbitrary. It follows from (5) that

$$\langle \lambda, v - \phi \rangle = \langle \lambda, v - u \rangle \geq 0.$$

□

Remark 1 (Existence of optimal multiplier with a nonpositive obstacle $\phi \in V_0$). If we would deal with an obstacle $\phi \in V_0$, the existence of optimal multiplier could be proved as follows: Once again, the relation (14) defines a linear continuous functional λ in V_0 such that u minimizes the perturbed functional J_λ defined by (8). Since $\phi \in K$, we can choose $v = \phi$ as well as $v = 2u - \phi$ and apply the inequality (5), which implies that $\langle \lambda, u - \phi \rangle = 0$. Subsequently, it follows from (8) that $J_\lambda(u) = J(u)$. The condition of nonnegativity from definition (6) is also fulfilled, it is sufficient to apply the inequality (5) to a function $u + v$, where $v \in V_0$ and $v \geq 0$ a.e. in $(0, 1)$.

Remark 2 (Representation of (13) by a function $\lambda \in L^2(0, 1)$). If $u \in H_0^1(0, 1) \cap H^2(0, 1)$, then integration by parts yields

$$\langle \lambda, w \rangle = - \int_0^1 u'' v dx - \int_0^1 f v dx + t \left[- \int_0^1 u'' u dx - \int_0^1 f u dx \right] = \int_0^1 \lambda v dx + t \int_0^1 \lambda u dx,$$

where

$$\lambda = -(u'' + f). \quad (15)$$

In this case, the condition $\phi \in H^2(0, 1)$ have to be fulfilled.

Remark 3 (Saddle point problem interpretation). The pair (λ, u) is apparently a saddle point of the perturbed functional satisfying

$$J_\lambda(u) = \sup_{\mu \in \Lambda} \inf_{v \in V_0} J_\mu(v) = \inf_{v \in V_0} \sup_{\mu \in \Lambda} J_\mu(v) = J(u).$$

For more details, you can see e.g. [5, p. 107-109].

2 Benchmark with known analytical solution

We derive an exact solution of Problem 1 assuming negative constant functions f and ϕ . The resulting solution is displayed in Figure 2 for the case of active obstacle. A mechanical intuition suggests that for small values (considered in absolute value) of acting force f , there will be no contact with the obstacle and there will be a contact on a subset of interval $(0, 1)$ located symmetrically around the value $x = 1/2$ for higher values of f . Note that the solution of Problem 1 with inactive obstacle is equivalent to the solution



Figure 2: Benchmark setup: Constant forces f pressing continuum against a constant lower obstacle ϕ , exact displacement u (left) and construction of exact displacement u in detail (right).

of (1) - (2) and it reads

$$u(x) = \frac{f}{2}(x - x^2). \quad (16)$$

The minimal value of u on interval $(0,1)$ is attained at $x = 1/2$ and the inactive obstacle condition $u(1/2) > \phi$ is satisfied for

$$|f| < 8|\phi|. \quad (17)$$

Then, the corresponding energy reads

$$J(u) := -\frac{f^2}{24}. \quad (18)$$

The obstacle is active if

$$|f| \geq 8|\phi|, \quad (19)$$

and the solution has the following form

$$u(x) = \begin{cases} -\frac{f}{2}x^2 + \frac{\phi + \frac{f}{2}(\frac{1}{2}-r)^2}{\frac{1}{2}-r}x & \text{if } x \in [0, \frac{1}{2}-r) \\ \phi & \text{if } x \in [\frac{1}{2}-r, \frac{1}{2}+r] \\ -\frac{f}{2}(x-1)^2 - \frac{\phi + \frac{f}{2}(\frac{1}{2}-r)^2}{\frac{1}{2}-r}(x-1) & \text{if } x \in (\frac{1}{2}+r, 1] \end{cases}$$

for unknown parameter $r \in [0, \frac{1}{2}]$. The parameter r determines the active contact set $[\frac{1}{2}-r, \frac{1}{2}+r]$ and its value can be determined from the minimum of energy

$$J(u) = \frac{[\phi + \frac{f}{2}(\frac{1}{2}-r)^2]^2}{\frac{1}{2}-r} - 2[\phi + \frac{f}{2}(\frac{1}{2}-r)^2]f(\frac{1}{2}-r) + \frac{2f^2}{3}(\frac{1}{2}-r)^3 - 2fr\phi$$

over all value of $r \in [0, \frac{1}{2}]$. The minimal energy

$$J(u) = f\phi(\frac{4}{3}\sqrt{\frac{2\phi}{f}} - 1) \quad (20)$$

is achieved for the argument

$$r = \frac{1}{2} - \sqrt{\frac{2\phi}{f}}. \quad (21)$$

Therefore, the solution of the problem with the active obstacle reads

$$u(x) = \begin{cases} -\frac{f}{2}x^2 - \sqrt{2\phi f}x & \text{if } x \in [0, \sqrt{\frac{2\phi}{f}}) \\ \phi & \text{if } x \in [\sqrt{\frac{2\phi}{f}}, 1 - \sqrt{\frac{2\phi}{f}}] \\ -\frac{f}{2}(x-1)^2 + \sqrt{2\phi f}(x-1) & \text{if } x \in (1 - \sqrt{\frac{2\phi}{f}}, 1] \end{cases} \quad (22)$$

Figure 3 provides few numerical approximations of u , see Section 5 for details. The first-order derivative

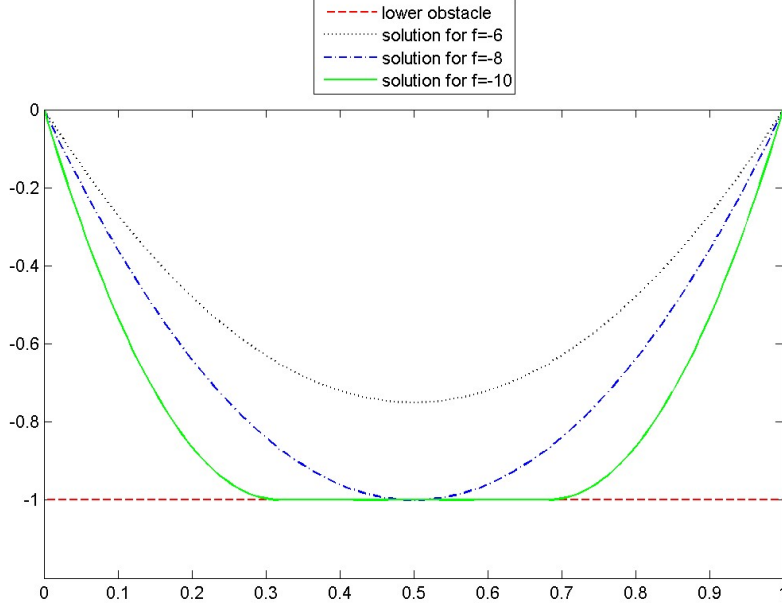


Figure 3: Solutions for problems with loadings $f \in \{-6, -8, -10\}$ and $\phi = -1$.

$$u'(x) = \begin{cases} -fx - \sqrt{2\phi f} & \text{if } x \in \left[0, \sqrt{\frac{2\phi}{f}}\right) \\ 0 & \text{if } x \in \left[\sqrt{\frac{2\phi}{f}}, 1 - \sqrt{\frac{2\phi}{f}}\right] \\ -f(x-1) + \sqrt{2\phi f} & \text{if } x \in \left(1 - \sqrt{\frac{2\phi}{f}}, 1\right] \end{cases} \quad (23)$$

is continuous everywhere. It is not difficult to show that

$$u''(x) = \begin{cases} -f & \text{if } x \in \left(0, \sqrt{\frac{2\phi}{f}}\right) \\ 0 & \text{if } x \in \left(\sqrt{\frac{2\phi}{f}}, 1 - \sqrt{\frac{2\phi}{f}}\right) \\ -f & \text{if } x \in \left(1 - \sqrt{\frac{2\phi}{f}}, 1\right) \end{cases} \quad (24)$$

is the second-order weak derivative of (22). Thus, it follows from (15) that the optimal multiplier for our benchmark problem reads

$$\lambda(x) = \begin{cases} 0 & \text{if } x \in \left(0, \sqrt{\frac{2\phi}{f}}\right) \\ -f & \text{if } x \in \left(\sqrt{\frac{2\phi}{f}}, 1 - \sqrt{\frac{2\phi}{f}}\right) \\ 0 & \text{if } x \in \left(1 - \sqrt{\frac{2\phi}{f}}, 1\right) \end{cases} \quad (25)$$

so that it is a piecewise constant function.

3 Functional a posteriori error estimate in 1D - general part

We are interested in analysis and numerical properties of the a posteriori error estimate in the energetic norm

$$\|v\|_E := \left(\int_0^1 (v')^2 dx \right)^{\frac{1}{2}}.$$

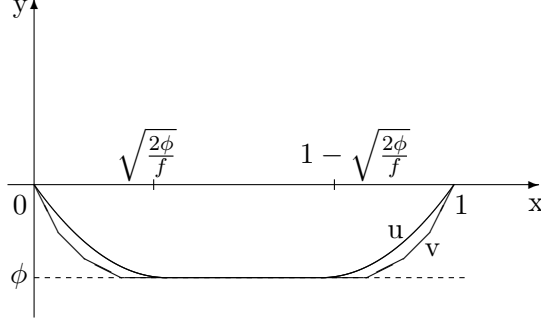


Figure 4: Contact zone of the discrete solution v covers the contact zone of the exact solution.

This section is based on results of P. Neittaanmäki and S. Repin [5]. We apply the general framework to one dimensional case, but try to achieve exact integration rules wherever it is possible. As well as in [5], it is simple to see that

$$J(v) - J(u) = \frac{1}{2} \int_0^1 [(v - u)']^2 dx + \int_0^1 u'(v - u)' dx - \int_0^1 f(v - u) dx \quad (26)$$

and (5) implies the energy estimate

$$\frac{1}{2} \|v - u\|_E^2 \leq J(v) - J(u) \quad \text{for all } v \in K. \quad (27)$$

Estimate (27) can only be tested for problems with known exact solution $u \in K$. One problem with known exact solution will be given in Section 2.

Remark 4 (Sharpness of estimate (27)). It is clear from (26), the estimate (27) turns into equality if

$$\langle \lambda, v - u \rangle = \int_0^1 u'(v - u)' dx - \int_0^1 f(v - u) dx = 0 \quad \text{for all } v \in K. \quad (28)$$

This situation always occurs if $\lambda = 0$. Then, (14) implies that u is a solution of Problem 1 in the whole space V_0 . This corresponds to a linear problem without any obstacle. However, the estimate (27) can turn into equality also for the active obstacle. Indeed, (28) rewrites as

$$\langle \lambda, v - u \rangle = -f \int_{\sqrt{\frac{2\phi}{f}}}^{1 - \sqrt{\frac{2\phi}{f}}} (v - u) dx = 0, \quad (29)$$

if the contact zone of an approximate solution $v \in K$ includes whole contact zone $\left[\sqrt{\frac{2\phi}{f}}, 1 - \sqrt{\frac{2\phi}{f}}\right]$ of exact solution u , see Figure 4.

Further, we substitute (9) into (27) to obtain the estimate

$$J(v) - J(u) \leq J(v) - J_\mu(u_\mu) \quad \text{for all } \mu \in \Lambda. \quad (30)$$

In practical computations, $u_\mu \in \Lambda$ will be approximated by $u_{\mu,h} \in V_{0,h}$ from some finite dimensional subspace $V_{0,h} \subset V_0$. Therefore, it holds

$$J_\mu(u_{\mu,h}) \geq J_\mu(u_\mu)$$

and $J_\mu(u_{\mu,h})$ can not replace $J_\mu(u_\mu)$ in (30) so that the inequality holds. Therefore, estimate (30) is practically not interesting. To avoid this difficulty, we establish the following problem:

Problem 3 (Dual perturbed problem). Find $\tau_\mu^* \in Q_{f\mu}^* \subset L^2(0, 1)$ such that

$$J_\mu^*(\tau_\mu^*) = \sup_{q^* \in Q_{f\mu}^*} J_\mu^*(q^*), \quad (31)$$

where

$$J_\mu^*(q^*) = -\frac{1}{2} \int_0^1 (q^*)^2 dx + \langle \mu, \phi \rangle \quad (32)$$

and

$$Q_{f\mu}^* := \left\{ q^* \in L^2(0, 1) : \langle \mu, v \rangle = \int_0^1 q^* v' dx - \int_0^1 f v dx \quad \text{for all } v \in V_0 \right\}. \quad (33)$$

Lemma 2. It holds

$$\sup_{q^* \in Q_{f\mu}^*} J_\mu^*(q^*) = J_\mu^*(u'_\mu) = J_\mu(u_\mu).$$

Proof. As a consequence of (7), it holds that $u'_\mu \in Q_{f\mu}^*$. Let $w \in Q_{f\mu}^*$ is arbitrary. Since

$$J_\mu^*(w) = J_\mu^*(u'_\mu) - \int_0^1 u'_\mu(w - u'_\mu) dx - \frac{1}{2} \int_0^1 (w - u'_\mu)^2 dx$$

and $\int_0^1 u'_\mu(w - u'_\mu) dx = 0$ in consequence of $u'_\mu, w \in Q_{f\mu}^*$, we deduce that $J_\mu^*(u'_\mu)$ is supremum of dual perturbed functional J_μ^* . Finally, it is not difficult to verify that $J_\mu^*(u'_\mu) = J_\mu(u_\mu)$. \square

Corollary 1. If we choose

$$\mu = \lambda,$$

it holds

$$J_\lambda(u) = \inf_{v \in V_0} J_\lambda(v) = \sup_{q^* \in Q_{f\lambda}^*} J_\lambda^*(q^*) = J_\lambda^*(u') = J(u).$$

It follows from Lemma 2, we can replace the inequality (30) by

$$J(v) - J(u) \leq J(v) - \sup_{q^* \in Q_{f\mu}^*} J_\mu^*(q^*) \leq J(v) - J_\mu^*(q^*), \quad (34)$$

where $q^* \in Q_{f\mu}^*$ is arbitrary. It is easy to see that we can rewrite (34) to form

$$J(v) - J(u) \leq \int_0^1 \left[\frac{1}{2} (v')^2 - f v \right] dx + \int_0^1 \frac{1}{2} (\tau^*)^2 dx + \frac{1}{2} \int_0^1 [(q^*)^2 - (\tau^*)^2] dx - \langle \mu, \phi \rangle, \quad (35)$$

where $\tau^* \in L^2(0, 1)$ is arbitrary.

From now, we only consider more special case:

$$\mu \in \Lambda := \{ \mu \in L^2(0, 1) : \mu \geq 0 \text{ a.e. in } (0, 1) \}.$$

Then,

$$\langle \mu, v \rangle = \int_0^1 \mu v dx.$$

The application of estimate (35) is possible, the only limitation is to satisfy the constrain $q^* \in Q_{f\mu}^*$. In the following, we recall the technique of [5] in order to replace the constrain by a special penalty term. We obtain

$$J(v) - J(u) \leq \frac{1+\beta}{2} \int_0^1 (v' - \tau^*)^2 dx + \frac{1}{2} \left(1 + \frac{1}{\beta} \right) \int_0^1 (q^* - \tau^*)^2 dx + \int_0^1 \mu(v - \phi) dx,$$

where $\beta > 0$.

Since $q^* \in Q_{f\mu}^*$ is arbitrary, we can take the error estimate

$$J(v) - J(u) \leq \frac{1+\beta}{2} \int_0^1 (v' - \tau^*)^2 dx + \frac{1}{2} \left(1 + \frac{1}{\beta}\right) [d^2(\tau^*, Q_{f\mu}^*)] + \int_0^1 \mu(v - \phi) dx,$$

where

$$d^2(\tau^*, Q_{f\mu}^*) := \inf_{q^* \in Q_{f\mu}^*} \int_0^1 (q^* - \tau^*)^2 dx.$$

If $(\tau^*)' \in L^2(0, 1)$, i.e. $\tau^* \in H^1(0, 1)$, we can infer, analogously as in [5], that

$$d^2(\tau^*, Q_{f\mu}^*) \leq C^2 \|(\tau^*)' + f + \mu\|_{L^2(\Omega)}^2,$$

where a constant $C > 0$ originates from the Friedrichs inequality

$$\int_0^1 u^2 dx \leq C^2 \int_0^1 (u')^2 dx \quad \forall u \in H_0^1(0, 1).$$

Since, in our problem, we can put $C = 1$, we obtain ultimately the following error estimate:

$$J(v) - J(u) \leq \frac{1+\beta}{2} \int_0^1 (v' - \tau^*)^2 dx + \frac{1}{2} \left(1 + \frac{1}{\beta}\right) \|(\tau^*)' + f + \mu\|_{L^2(\Omega)}^2 + \int_0^1 \mu(v - \phi) dx, \quad (36)$$

where the right-hand side of (36) is so called majorant $\mathcal{M} = \mathcal{M}(v, f, \phi; \beta, \mu, \tau^*)$.

Remark 5 (Optimal majorant parameters). Let $\mu = \lambda$, $\tau^* = u'$ and $\beta \rightarrow 0$. Then, it is not difficult to show that the inequality in (36) changes to equality, i.e. the majorant on right-hand side of (36) defines the difference of energies $J(v) - J(u)$ exactly.

4 Majorant minimization

For given solution approximation v , loading f and the obstacle ϕ , the majorant \mathcal{M} represents a convex functional in each of unknown variables β, μ, τ^* . Our goal is to find such variables $\beta_{\text{opt}}, \mu_{\text{opt}}$ and τ_{opt}^* that minimize the majorant \mathcal{M} .

Problem 4 (Majorant minimization problem). Let $v \in K$, $f \in L^2(0, 1)$, $\phi < 0$ be given. Find optimal $\beta_{\text{opt}} > 0$, $\mu_{\text{opt}} \in \Lambda$ and $\tau_{\text{opt}}^* \in H^1(0, 1)$ such that

$$\mathcal{M}(v, f, \phi; \beta_{\text{opt}}, \mu_{\text{opt}}, \tau_{\text{opt}}^*) = \min_{\beta, \mu, \tau^*} \mathcal{M}(v, f, \phi; \beta, \mu, \tau^*).$$

Algorithm 1 (Majorant minimization algorithm). Let $k = 0$ and let $\beta_k > 0$ and $\mu_k \in \Lambda$ be given. Then:

- (a) find $\tau_{k+1}^* \in H^1(0, 1)$ such that

$$\mathcal{M}(v, f, \phi; \beta_k, \mu_k, \tau_{k+1}^*) = \min_{\tau^* \in H^1(0, 1)} \mathcal{M}(v, f, \phi; \beta_k, \mu_k, \tau^*),$$

- (b) find $\mu_{k+1} \in \Lambda$ such that

$$\mathcal{M}(v, f, \phi; \beta_k, \mu_{k+1}, \tau_{k+1}^*) = \min_{\mu \in \Lambda} \mathcal{M}(v, f, \phi; \beta_k, \mu, \tau_{k+1}^*),$$

- (c) find $\beta_{k+1} > 0$ such that

$$\mathcal{M}(v, f, \phi; \beta_{k+1}, \mu_{k+1}, \tau_{k+1}^*) = \min_{\beta > 0} \mathcal{M}(v, f, \phi; \beta, \mu_{k+1}, \tau_{k+1}^*),$$

- (d) set $k = k + 1$ and repeat (a)-(c) until convergence.

The minimization in step (c) leads to the explicit relation

$$\beta_{k+1} = \frac{\|(\tau_{k+1}^*)' + f + \mu_{k+1}\|_{L^2(0,1)}}{\|v' - \tau_{k+1}^*\|_{L^2(0,1)}}. \quad (37)$$

The minimization in step (a) is equivalent to the following variational equation : Find $\tau_{k+1}^* \in H^1(0,1)$ such that

$$\begin{aligned} (1 + \beta_k) \int_0^1 \tau_{k+1}^* w dx + \left(1 + \frac{1}{\beta_k}\right) \int_0^1 (\tau_{k+1}^*)' w' dx \\ = (1 + \beta_k) \int_0^1 v' w dx - \left(1 + \frac{1}{\beta_k}\right) \int_0^1 (f + \mu_k) w' dx \quad \text{for all } w \in H^1(0,1). \end{aligned} \quad (38)$$

In later numerical experiments, we search a solution of (38) in a finite-element space $V_h \subset H^1(0,1)$. By introducing an interval partition with nodes

$$0 = x_1 < x_2 < \dots < x_n = 1, \quad (39)$$

we define V_h as the space of functions continuous on $[0,1]$ and linear on the interval $[x_j, x_{j+1}]$, $j = 1, \dots, n-1$. In usual nodal basis ψ_j , $j = 1 \dots n$, the relation (38) rewrites as a linear system of equations in matrix form

$$\left[(1 + \beta_k)M + \left(1 + \frac{1}{\beta_k}\right) A \right] y = (1 + \beta_k)b - \left(1 + \frac{1}{\beta_k}\right) c, \quad (40)$$

for unknown coefficients $y = (y_1, \dots, y_n) \in R^n$ representing $\tau_{k+1}^* = \sum_{j=1}^n y_j \psi_j$. Here, $M = (m_{ij})$ is a mass matrix, $A = (a_{ij})$ is a stiffness matrix,

$$m_{ij} = \int_0^1 \psi_i \psi_j dx, \quad a_{ij} = \int_0^1 \psi_i' \psi_j' dx$$

and b and c are n - dimensional vectors

$$b_i = \int_0^1 v' \psi_i dx, \quad c_i = \int_0^1 (f + \mu_k) \psi_i' dx$$

for $i, j = 1 \dots n$.

The minimization in step (b) is equivalent to the variational inequality: Find $\mu_{k+1} \in \Lambda$ such that

$$\int_0^1 \left[\left(1 + \frac{1}{\beta_k}\right) [\mu_{k+1} + (\tau_{k+1}^*)' + f] + v - \phi \right] (w - \mu_{k+1}) dx \geq 0 \quad \text{for all } w \in \Lambda.$$

In numerical experiments, we look for $\mu_{k+1} \in \Lambda$ in the space of piecewise constant functions defined on (39). Under the assumption of piecewise linear functions ϕ and v and piecewise constant functions f and $(\tau^*)'$ on (39) with given values

$$\phi(x_j), \phi(x_{j+1}), \quad v(x_j), v(x_{j+1}), \quad f(x_{j+\frac{1}{2}}), \quad (\tau_{k+1}^*)'(x_{j+\frac{1}{2}}),$$

the exact minimizer reads

$$\mu_{k+1}(x_{j+\frac{1}{2}}) = \left(-(\tau_{k+1}^*)'(x_{j+\frac{1}{2}}) - f(x_{j+\frac{1}{2}}) - \frac{v(x_j) + v(x_{j+1}) - \phi(x_j) - \phi(x_{j+1})}{2 \left(1 + \frac{1}{\beta_k}\right)} \right)^+, \quad (41)$$

where $(\cdot)^+ = \max\{0, \cdot\}$.

5 Numerical experiments

Numerical approximation v of the exact solution u from (22) is searched as a piecewise linear function defined on the partition (39) and constructed by using the Uzawa algorithm.

Algorithm 2 (Uzawa algorithm).

1. Set the initial Lagrange multiplier $\mu_0 = 0$.
2. Start of the loop: for $k = 1, 2, \dots$ do until convergence:
3. Find $v_k \in H_0^1(0, 1)$ such that $J_{\mu_k}(v_k) \rightarrow \min$.
4. Set $\mu_k = (\mu_{k-1} + \rho(v_k - \phi))^+$.
5. End of the loop.
6. Output $v = v_k$ and $\mu = \mu_k$.

The minimization in step 3. of Algorithm 2 is equivalent to the following variational equation: Find $v_k \in H_0^1(0, 1)$ such that

$$\int_0^1 v_k' w' dx = \int_0^1 (f + \mu_k) w dx \quad \text{for all } w \in H_0^1(0, 1).$$

By using the partition (39) and corresponding nodal basis, we can represent the k -th iteration v_k by linear combination of the basis functions $\psi_2, \dots, \psi_{n-1}$, i.e. $v_k = \sum_{j=2}^{n-1} y_j \psi_j$. Then, the unknown coefficients y_2, \dots, y_{n-1} can be obtained by solving of a linear system of equations analogous to (40).

The convergence of Algorithm 2 depends on the choice of the scalar parameter ρ and it can be shown, see e.g. [?], that it always converges for $\rho \in (0, \rho_1)$ for some $\rho_1 > 0$. Here, we consider the case $f = -14$, choose $\rho = 10$ and run Algorithm 2 with 10000 iterations. The first iteration (v_1, μ_1) , the second iteration (v_2, μ_2) and the final (the 10000th) iteration (v, μ) are displayed in Figure 5.

Assuming the uniform mesh with 641 nodes (which correspond to 6 uniform refinements of an initial uniform mesh with 10 elements), we consider approximate solutions (v, μ) obtained by Algorithm 2 with 100, 1000, and 10000 iterations and we verify estimates (27) and (36). The results are reported in Tables 1, 2, 3. For cases with an inactive obstacle (for loadings $f \in \{-5, \dots, -8\}$), the energy estimate (27) is always the sharpest possible (see values 1.00 in the fourth column of each Table), which is known from Remark 4. Such cases are described by purely quadratic minimization problems, whose discrete solutions are obtained already after one iteration of the Uzawa Algorithm. In other cases with an active obstacle (for loadings $f \in \{-9, \dots, -18\}$), we a priori choose the numbers of iterations in the Uzawa Algorithm in a way, that:

100 iterations provide inaccurate approximations v on the given uniform mesh of exact solutions u ,

1000 iterations provide more accurate approximations v on the given uniform mesh of exact solutions u ,

10000 iterations provide very accurate approximations v on the given uniform mesh of exact solutions u .

The majorant minimization algorithm is run with a high number of iterations (10000 in all experiments) in order to achieve the sharpest possible estimate (36) (this corresponds to values around 1.00 in the last column of each Table). We note that the functional majorant provides a sharp estimate of the difference of discrete and exact energies, no matter what quality of the approximation v above we consider.

Remark 6 (Update of β). The experiments showed that the update of β in the step c) of Algorithm 1 should not be called in every iteration. It turns out useful to call steps a) and b) repeatedly and run step c) only after variables τ^* and μ stabilize. We updated β during the 5000th and the final 10000th iterations.

The iterations of the majorant minimization algorithm are displayed in Figure 6. We consider initial setup $\beta_0 = 1, \mu_0 = 0$ and the inaccurate approximation v provided by 100 iterations of the Uzawa algorithm (taken from above). The majorant minimization algorithm with 10000 iterations provides a good quality of μ as well as of τ^* (see Remark 5).

Here, we are not interested in a fast and efficient majorant optimization, new strategies combined with effective minimization known for linear elliptic problems [7, 6] will be developed in forthcoming papers.

Acknowledgment

Both author acknowledge the support of the European Regional Development Fund in the Centre of Excellence project IT4Innovations (CZ.1.05/1.1.00/02.0070) and by the project SPOMECH - Creating a multi-disciplinary R&D team for reliable solution of mechanical problems, reg. no. CZ.1.07/2.3.00/20.0070 within Operational Programme 'Education for competitiveness' funded by Structural Funds of the European Union and state budget of the Czech Republic. Authors would also like to thank to S. Repin (St. Petersburg), J. Kraus (Linz), D. Pauli (Duisburg-Essen) and O. Vlach (Ostrava) for discussions.

References

- [1] *D. Braess, R. H. W. Hoppe, J. Schöberl*: A posteriori estimators for obstacle problems by the hypercircle method. *Comp. Visual. Sci.* 11, 2008, 351-362.
- [2] *R. Glowinski*: Lectures on numerical methods for non-linear variational problems. Springer-Verlag, 1980.
- [3] *R. Glowinski, J. L. Lions, R. Trémoières*: Numerical analysis of variational inequalities. North-Holland, 1981.
- [4] *J. L. Lions, G. Stampacchia*: Variational inequalities. *Comm. Pure Appl. Math.*, XX(3), 1967, 493-519.
- [5] *P. Neittaanmäki, S. Repin*: Reliable methods for computer simulation (error control and a posteriori estimates). Elsevier, 2004.
- [6] *J. Kraus, S. Tomar*: Algebraic multilevel iteration method for lowest-order Raviart-Thomas space and applications. *Int. J. Numer. Meth. Engng.* 86, 2011, 1175-1196.
- [7] *J. Valdman*: Minimization of functional majorant in a posteriori error analysis based on $H(\text{div})$ multigrid-preconditioned CG method. *Advances in Numerical Analysis*, 2009.

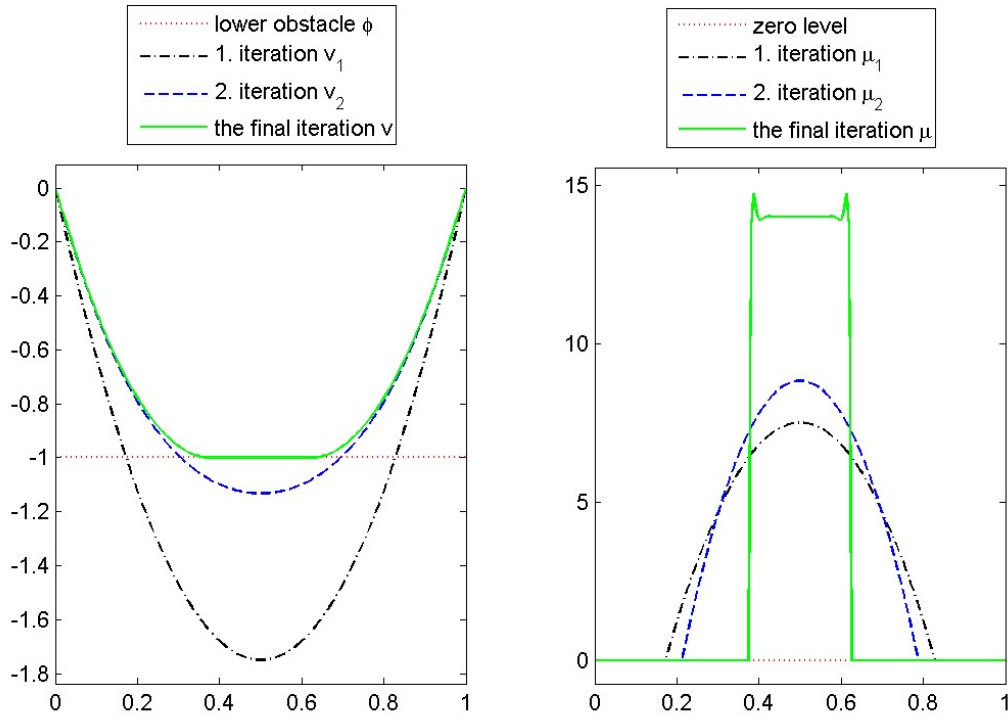


Figure 5: The first, the second and the final (the 10000th) iterations of the Uzawa algorithm for $f = -14$.

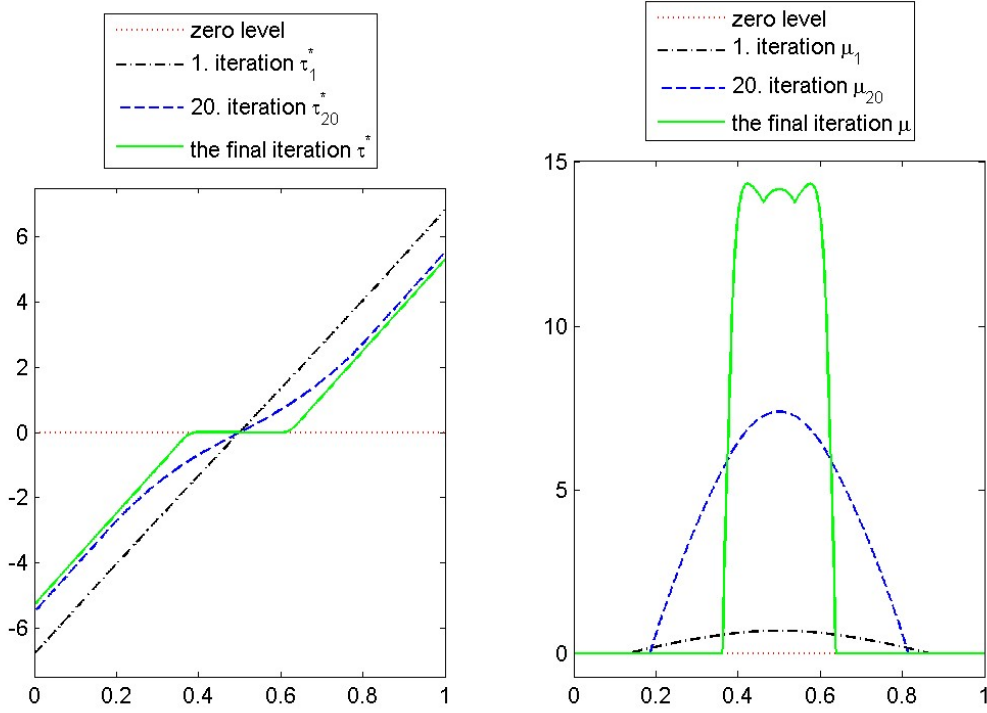


Figure 6: The first, the twentieth and the final (the 10000th) iterations of the majorant minimization algorithm for $f = -14$.

f	$\frac{1}{2}\ v - u\ _E^2$	$J(v) - J(u)$	$\sqrt{\frac{J(v)-J(u)}{\frac{1}{2}\ v-u\ _E^2}}$	$\mathcal{M}(v, \dots)$	$\sqrt{\frac{\mathcal{M}(v, \dots)}{J(v)-J(u)}}$
-5	2.54e-006	2.54e-006	1.00	2.55e-006	1.00
-6	3.66e-006	3.66e-006	1.00	3.67e-006	1.00
-7	4.98e-006	4.98e-006	1.00	4.99e-006	1.00
-8	6.51e-006	6.51e-006	1.00	6.52e-006	1.00
-9	2.27e-005	2.27e-005	1.00	2.39e-005	1.03
-10	6.49e-005	6.86e-005	1.03	7.41e-005	1.04
-11	8.25e-005	9.91e-005	1.10	1.06e-004	1.04
-12	8.57e-005	9.99e-005	1.08	1.07e-004	1.04
-13	8.42e-005	1.13e-004	1.16	1.20e-004	1.03
-14	8.73e-005	3.69e-004	2.06	3.75e-004	1.01
-15	8.86e-005	6.44e-004	2.70	6.51e-004	1.00
-16	1.02e-004	9.91e-004	3.11	9.98e-004	1.00
-17	1.13e-004	1.26e-003	3.34	1.27e-003	1.00
-18	1.24e-004	1.54e-003	3.53	1.55e-003	1.00

Table 1: Verification of majorant and energy estimates for problems with various f computed on an uniform mesh with 641 nodes. Discrete solutions v is computed by 100 iterations of the Uzawa algorithm.

f	$\frac{1}{2}\ v - u\ _E^2$	$J(v) - J(u)$	$\sqrt{\frac{J(v)-J(u)}{\frac{1}{2}\ v-u\ _E^2}}$	$\mathcal{M}(v, \dots)$	$\sqrt{\frac{\mathcal{M}(v, \dots)}{J(v)-J(u)}}$
-5	2.54e-006	2.54e-006	1.00	2.55e-006	1.00
-6	3.66e-006	3.66e-006	1.00	3.67e-006	1.00
-7	4.98e-006	4.98e-006	1.00	4.99e-006	1.00
-8	6.51e-006	6.51e-006	1.00	6.52e-006	1.00
-9	9.04e-006	9.49e-006	1.02	9.83e-006	1.02
-10	1.00e-005	2.36e-005	1.53	2.39e-005	1.01
-11	1.19e-005	2.72e-005	1.51	2.76e-005	1.01
-12	1.33e-005	2.90e-005	1.48	2.94e-005	1.01
-13	1.53e-005	3.96e-005	1.61	4.01e-005	1.01
-14	1.73e-005	4.79e-005	1.66	4.85e-005	1.01
-15	1.88e-005	5.61e-005	1.73	5.69e-005	1.01
-16	2.07e-005	5.51e-005	1.63	5.59e-005	1.01
-17	2.24e-005	6.01e-005	1.64	6.10e-005	1.01
-18	2.48e-005	6.94e-005	1.67	7.03e-005	1.01

Table 2: Verification of majorant and energy estimates for problems with various f computed on an uniform mesh with 641 nodes. Discrete solutions v is computed by 1000 iterations of the Uzawa algorithm.

f	$\frac{1}{2}\ v - u\ _E^2$	$J(v) - J(u)$	$\sqrt{\frac{J(v)-J(u)}{\frac{1}{2}\ v-u\ _E^2}}$	$\mathcal{M}(v, \dots)$	$\sqrt{\frac{\mathcal{M}(v, \dots)}{J(v)-J(u)}}$
-5	2.54e-006	2.54e-006	1.00	2.54e-006	1.00
-6	3.66e-006	3.66e-006	1.00	3.66e-006	1.00
-7	4.98e-006	4.98e-006	1.00	4.98e-006	1.00
-8	6.51e-006	6.51e-006	1.00	6.51e-006	1.00
-9	7.78e-006	8.05e-006	1.02	8.10e-006	1.00
-10	9.11e-006	9.79e-006	1.04	9.88e-006	1.00
-11	1.05e-005	1.10e-005	1.02	1.11e-005	1.00
-12	1.20e-005	1.29e-005	1.04	1.30e-005	1.00
-13	1.35e-005	1.42e-005	1.03	1.44e-005	1.00
-14	1.51e-005	1.60e-005	1.03	1.61e-005	1.00
-15	1.68e-005	1.78e-005	1.03	1.79e-005	1.00
-16	1.84e-005	2.01e-005	1.04	2.03e-005	1.01
-17	2.02e-005	2.16e-005	1.03	2.18e-005	1.00
-18	2.20e-005	2.39e-005	1.04	2.42e-005	1.01

Table 3: Verification of majorant and energy estimates for problems with various f computed on an uniform mesh with 641 nodes. Discrete solutions v is computed by 10000 iterations of the Uzawa algorithm.